

# We are IntechOpen, the world's leading publisher of Open Access books Built by scientists, for scientists

5,000

Open access books available

124,000

International authors and editors

140M

Downloads

Our authors are among the

154

Countries delivered to

TOP 1%

most cited scientists

12.2%

Contributors from top 500 universities



WEB OF SCIENCE™

Selection of our books indexed in the Book Citation Index  
in Web of Science™ Core Collection (BKCI)

Interested in publishing with us?  
Contact [book.department@intechopen.com](mailto:book.department@intechopen.com)

Numbers displayed above are based on latest data collected.  
For more information visit [www.intechopen.com](http://www.intechopen.com)



# Gravitational Quantisation and Dark Matter

Allan Ernest  
Charles Sturt University  
Australia

## 1. Introduction

This chapter looks at the concept of gravitational quantisation and the intriguing possibility that it may enable understanding one of the most mysterious problems in astrophysics: the nature and origin of dark matter. The concept of gravitational quantisation is relatively new, and from the traditional quantum mechanical viewpoint it raises questions about the applicability of quantum mechanics to gravitational fields, and also questions about the applicability of quantum mechanics on macroscopic scales, because the quantisation states of gravitational fields are sometimes large. Quantum physics was after all, originally developed to describe the behaviour of electrons in atoms and quickly became the recognised way to accurately model the physics of atomic-sized systems. Although it was an obvious extension that the structure of nuclei, which were even smaller, could also be well described using a wave-mechanical approach, for many years this was the limited domain in which quantum theory operated. Nevertheless the success of applying quantum physics to nuclear phenomena showed (1) that quantum theory was appropriate to potentials other than electrical (in this case the strong nuclear force) and (2) that it provided a correct description of nature over a range of scales ( $< \sim 2$  fm for nuclear structure compared to  $> \sim 50$  pm for atoms). The success in modelling nuclear phenomena did not necessarily mean however that quantum theory was suitable for describing nature over all scales and that it applied to all other types of potentials. For example, the existence of a region where quantum physics breaks down and classical physics takes over still remains a debated issue, but if such a region exists, at what scale does it happen? And secondly, for what other potentials or pseudo-potentials might quantum theory be valid and how would this validity be demonstrated?

With respect to the first question, we argue that there are at present no experiments that invalidate quantum theory at any scale, and that quantum-based predictions of classical or macroscopic measurements are expected to equally agree with those of classical calculations, provided careful attention is paid to effects such as decoherence (Zurek, 1981, 1982, Chou et al., 2011, Lamine et al., 2011, Jaekel et al., 2006, Schlosshauer, 2007). Indeed isolating a consistent value for the scale of the so-called mesoscopic region between the quantum and classical domain, above which classical theory would dominate, has proved elusive and experiments have continued to demonstrate the applicability of quantum physics at macroscopic scales. However, as the many newly-observed macroscopic quantum phenomena demonstrate, this does not preclude the possibility that quantum theory may lead to additional novel macroscopic phenomena that have no classical analogue. Examples

include experiments involving superconductivity and superconducting interference devices, and the experiments with entangled photons, atoms and molecules (Nakamura et al., 1999, Ketterle, 2002, Van der Wal et al., 2000, Zbinden et al., 2001, Schmitt-Manderbach et al., 2007).

With respect to the second point, recent experiments have also observed quantum effects in potentials and pseudo potentials other than electromagnetic or nuclear. In seminal work by Nesvizhevsky et al., 2002, quantised states of the gravitational field were observed in the laboratory. These remarkable experiments demonstrate for the first time that particles form gravitational eigenstates in gravitational potential wells, and hence that particles in gravitational potentials conform to the laws of quantum physics in the same way that electrons do in the electrical potentials around nuclei (despite any apparent but ongoing inconsistency between quantum mechanics and general relativity). If relatively pure gravitational quantum eigenstates can form in a laboratory situation then the question arises as to whether such eigenstates might exist naturally elsewhere in the universe, and if so, what their theoretical properties might be.

Research in the area of quantum gravity has been active for some time (for general reviews see DeWitt and Esposito, 2007, Rovelli, 2008 and Woodard, 2009). It should be noted that the aim in this chapter is not to develop a theory of quantum gravity. Quantum gravity seeks to produce a unified theory of quantum physics and general relativity under all conditions, particularly in regions of strong gravity where classical Newtonian approaches break down. Such a theory does not yet exist and is not needed in the current context, where a Newtonian formulation of gravitational quantum theory is used. The purpose here is to examine properties of the predicted quantum based eigenstates that exist predominantly in the weak gravity regions of (possibly deep) gravitational wells and to study the behaviour of particles in these regions using the traditional quantum eigenspectral decomposition of the particle wavefunctions in terms of their energy eigenstate basis vectors. That is, we do not include eigenstates that might have significant amplitude fractions in regions of strong gravity such as near black holes (and such states should not be needed as they form a small fraction of the eigenspectral decomposition for particles in weak gravity regions), and we assume that those states that are included in the decomposition may be approximated by ignoring any small fraction of their eigenstate function that does encroach on such regions. It will turn out that the use of a quantum gravitational approach introduces novel properties to particles that enable dark matter to arise as a natural consequence of cosmic evolution without the need for new particles or physics beyond traditional quantum theory. Coincidentally we will see that not only can gravitational quantisation potentially solve the dark matter problem, but also that it compels the introduction of a new paradigm for the macroscopic description of particles and their interaction properties.

The first evidence that dark matter might exist appeared over 70 years ago with Zwicky's observations of high rotation velocities of galaxies in the Virgo cluster which pointed to excess unseen mass (Zwicky, 1937). About 30 years later (Rubin, 1970) showed that the orbital speeds of stars and gas within galaxies did not fall off with radial position in a Keplerian manner as expected, but maintained a constant velocity as far out as could be measured. These galactic rotation curves seemed to clearly show that galaxies also contained mass beyond that that would be expected from their visible component. Significantly this "missing" mass is not a small fraction of the visible component. Instead it

dominates, making over 80% of the expected 27% matter content of the universe, and much more than this in some galaxies. Because these controversial observations seemed inexplicable and had such radical implications for the understanding of the universe they were initially treated with scepticism. Evidence has continued however to point to a universe whose dominant matter content remains a mystery. Strong evidence supporting this hypothesis also comes from observations of gravitational lensing and also those from the Wilkinson Microwave Anisotropy Probe (WMAP). These 'dark' particles are essentially invisible: as far as observations reveal, they do not radiate energy, are transparent to electromagnetic radiation and weakly interacting with ordinary (baryonic) particles.

Cosmologists' currently favoured solution is the cold dark matter theory (CDM) or the more recent modification that includes dark energy, lambda cold dark matter (LCDM) (Primack, 2001). The theory is based then on the hypothetical existence of an as yet undiscovered weakly interacting elementary particle. Although no such particle is predicted from the standard model of particle physics, there are extensions to the standard model such as supersymmetry (Feng, 2010) that potentially have theoretically predicted particles that might function as long-lived weakly interacting particles. Given that such a particle exists, numerical simulations of LCDM have been developed, and these have been very successful in predicting the very large scale structure of the universe (see Croft and Estathiou, 1993, Colberg et al., 1997). In these simulations the structure of the universe grows by gravitational coalescence of dark matter particles to initially form small agglomerations that then combine in a process of hierarchical merging (Knebe, 1998, Diemand and Moore, 2009) to form the clusters and large galaxies seen today. Numerical simulations initially using particle masses of  $\sim 10^{41}$  kg (because of computational constraints) and later smaller masses both give similar and excellent prediction of large scale universal structure.

Despite the successes of LCDM cosmology on large scales, it faces some very serious challenges on the galactic scale and below (Kroupa et al., 2010). The problems have been so difficult that some cosmologists have questioned the validity of the entire LCDM theory. The numerical simulations of CDM produce steep cusp-like density profiles at low galactic halo radii, an overabundance of satellite galaxies and problems with the predicted angular momentum (ibid.). Additionally, the observation of fully formed galaxies like the Milky Way at very early times in cosmic history presents a formation mechanism problem since it is difficult to understand how this could have happened via hierarchical merging, a cornerstone of LCDM cosmology for understanding galaxy formation, in the limited time available (ibid.).

There have been several proposed alternate theories to the idea that the dark matter observations arise as the result of hidden mass. One group of these alternative solutions is based on the notion that the equations describing gravity on large scales may need to be modified. The idea, originally due to Milgrom (1983) - Modified Newtonian Dynamics or MOND has now many variations that include relativity and generalisations of quantum gravity. These theories all have the effect of modifying gravity in such a way as to explain the galactic rotation curves and thus also remove the need for the explanation of the dark matter observations in terms of unseen excess mass. However evidence that the "dark matter" observations are truly the result of the existence of extra unseen matter continues to grow and it has become increasingly difficult to explain dark matter in terms of modified gravity. One group of relatively recent observations compelling for the bona-fide existence

of dark matter are those of galactic cluster collisions such as the famous Bullet cluster, 1E 0657-56. In the Bullet cluster evidence is seen of the separation of dark matter from the visible components as a result of the collision. The dominant mass component, the dark matter, along with the individual galaxies within the cluster have passed through one another largely unaffected, but the gas components have interacted and are seen between the two now separated dark matter/galactic cluster components (Clowe et al., 2006).

The suggestion that gravitational quantisation might play a direct role in the solution to the dark matter problem was first made by Ernest (2001) and later using a fundamentally different approach by Chavda and Chavda (2002). In the former case (the approach in this chapter) Ernest considered the effects that the eigenspectral array describing the wavefunctions of traditional particles has on their interaction properties, while Chavda and Chavda consider the bound quantum eigenstate of two micro black holes and suggest that due to their binding, the constituent black holes of such a system will not lose mass in the expected manner (i.e from Hawking radiation). In this way micro black holes formed in the early universe could be still present today rather than having evaporated at earlier times and hence function as an alternative dark matter candidate like the neutralino.

## **2. Naturally occurring gravitational eigenstates: Quantum wavefunctions with limited eigenspectral range and the connection with dark matter**

### **2.1 Conditions for naturally occurring gravitational eigenstates**

Predicting the behaviour of particles in gravitational fields using quantum mechanics is in principle simple. One applies the non-relativistic Schrodinger equation to a Newtonian potential to yield its eigenstates and energies. Once the eigenstates are known, the temporal evolution of any particle in that potential is determined from the temporal evolution of the eigenspectral array that describes the initial wavefunction, essentially what is classically the initial conditions of the particle. Several authors have developed theoretical and numerical solutions to these types of equations under various conditions (Bernstein et al., 1998, Doran et al., 2005, Vachaspati, 2005, Gossel et al., 2010) and used them to make predictions about various physical phenomena ranging from astrophysical processes such as rates of accretion onto black holes, to understanding the behaviour of a gravitational Bose-Einstein condensate.

Very little work has been done however to investigate the potential existence or theoretical properties of gravitational eigenstates and their consequences for astrophysics (Ernest 2009a, 2009b). The simplest gravitational eigenstate system would feasibly consist of two neutral, spin-zero elementary-type particles in a bound state. The problem for such a system is that the binding energy is unrealistically small. For example, if the masses were  $\sim 10^{-27}$  kg, the most highly bound state, with principle quantum number  $n = 1$  has a binding energy of  $\sim -10^{-69}$  eV which is minuscule compared to typical universally pervading energies, for example, cosmic microwave background photons ( $\sim 2 \times 10^{-4}$  eV) or the observed dark energy component of  $\sim 1 \text{ GeV m}^{-3}$  (Tegmark et al., 2004).

The easiest way to increase the binding energy is to increase one or more of the two masses of this two component system. By pushing the component masses to 'grains' of  $\sim 10^{-13}$  kg each, the energy of the  $n = 1$  state becomes a healthy -10 eV. But there are things to consider than just the binding energy. Given typical densities of  $10^3 -$



$10^4 \text{ kg m}^{-3}$  for the masses, the physical size of each is  $\sim 10^{-6} \text{ m}$ . The initial and simplest mathematical approach involves two single point potentials and clearly requires that the ‘physical extent’ of the masses should not encroach into any significant fraction of the space occupied by the eigenfunction, otherwise the effective potential between the two changes, and the description in terms of a simple Schrödinger equation breaks down. For  $n = 1$ , the scale of the  $-10 \text{ eV}$  energy eigenstate above is  $\sim 10^{-19} \text{ m}$  so that this condition is clearly not satisfied. For higher  $n$  states, the position of the wavefunction is shifted to larger radii, which alleviates this difficulty, but the binding energy of the eigenstate approaches zero. One way to circumvent these difficulties is to consider a small elementary type particle (say of mass  $1.7 \times 10^{-27} \text{ kg}$ ) bound in the central potential well of a much larger mass and consider only large values of  $n$ , and particularly the high angular momentum states where  $l \sim n$  (see Table 1)

Central mass $M \text{ (kg)}$	$n$ value at eigenstate energy $\sim 1 \text{ eV}$	Eigenstate ‘size’ for $l \sim n \text{ (m)}$	Physical radius of central mass (m) assuming density $\sim 5 \times 10^3 \text{ kg m}^{-3}$
$10^{10}$	$7.6 \times 10^2$	$3.5 \times 10^{-9}$	$7.6 \times 10^1$
$10^{20}$	$7.6 \times 10^{12}$	$3.5 \times 10^1$	$1.6 \times 10^5$
$6 \times 10^{24} \text{ (} M_{\text{Earth}} \text{)}$	$4.6 \times 10^{17}$	$2.1 \times 10^6$	$6.4 \times 10^6$
$10^{30} \text{ (} M_{\text{Sun}} \text{)}$	$7.6 \times 10^{22}$	$3.5 \times 10^{11}$	$3.5 \times 10^8$
$10^{40}$	$7.6 \times 10^{32}$	$3.5 \times 10^{21}$	$7.6 \times 10^{11}$

Table 1. Eigenstate ‘size’ versus central mass size for a fixed binding energy ( $1 \text{ eV} \sim 5000 \text{ K}$ ) and ‘orbit mass’  $= 1.7 \times 10^{-27} \text{ kg}$ .

With a central point mass potential well, for a given fixed binding energy  $E_n$ , the quantum number  $n$  is proportional to the central mass  $M$ . (see solutions to equation (1) below). Additionally, for the high angular momentum states ( $l \sim n$ ), the average effective eigenstate radius and thickness are proportional to  $M$  and  $M^{1/2}$  respectively, while the physical size of the central mass grows only as  $M^{1/3}$ . Thus although the value of  $n$  required to form an eigenstate which ‘clears’ the physical extent of the central mass increases as the central mass is increased, the critical value of  $n$  required to do this corresponds to a more highly bound structure the larger  $M$  is. Thus by increasing the central mass sufficiently it is possible to obtain a well-bound structure and maintain an eigenstate which does not encroach on the physical extent of the central mass. This behaviour is illustrated in Table 1. What constitutes ‘well-bound’ is arguable, but for a binding energy of  $1 \text{ eV}$  and an ‘orbit mass’ of  $\sim 10^{-27} \text{ kg}$ , Table 1 shows that the required central mass needs to be of the order or greater than the mass of the Earth. Certainly for the solar mass ( $\sim 10^{30} \text{ kg}$ ) and above the condition is easily achieved and the analysis can be carried out using a single particle simple Newtonian-type Schrodinger equation.

2.2 Connection with dark matter

What connection does dark matter have with gravitational eigenstates? Quantum mechanics is simply an alternative way to model nature, most useful on small scales. But we do expect

that quantum physics should equally well model all classical macroscopic phenomena, predicting essentially identical results, a belief echoed in the correspondence principle. Yet quantum theory has already yielded many novel macroscopic non-classical phenomena, so could a quantum mechanical description of the motion of elementary particles in a galactic potential also yield new insights? Remarkably, a quantum description of gravitationally bound particles does indeed predict new and intriguing effects. The reason comes from the predictions that quantum theory makes about variations in the interaction cross sections of particles based on their eigenspectra, which can exhibit unique properties in the case of macroscopic gravity.

### 2.2.1 Cross sections and eigenspectra

The concept of describing interactions in terms of a cross section has been one of the most fundamental and useful in physics. Simply put, cross sections measure the effective area that one particle (the 'target' particle) presents to another (the 'bullet') when interacting. Additionally, it is a measure of the rate at which a reaction occurs. In the laboratory, measurements of cross sections are made using a localised 'beam' of bullets, measuring the rate at which they 'hit' the target, and performing an analysis generally based on the assumption of a uniform incoming 'plane wave' of particles. But whilst it may seem reasonable, there is an implicit assumption in this about the nature of wavefunctions representing the particles. There is also often an assumption that a measured cross section is somehow independent of all but the most evident characteristics of the wavefunctions representing the particles involved in the measurement.

Some aspects of the wavefunction that affect the cross section are obvious. For example classically the 'chance' (and hence rate) at which two particles placed in a box will interact depends on the size of the box. This is trivially allowed for in the experiment by including the 'beam intensity' in the analysis. Likewise no one finds it surprising that cross sections depend on temperature because it is clear we are changing the fundamental nature of the interaction. Importantly though, this represents a specific example of how the wavefunction characteristics, in this case the eigenspectral wavelengths, affect the relevant overlap integrals that determine the rate of reaction and the cross section. But there are also subtleties of the wavefunctional form that can lead to dramatic changes in the resulting cross section of a particular interaction. In short, the measured cross section for any interaction is intimately linked to the eigenspectral array of the wavefunctions representing the particles involved. If the eigenspectral array from which the particle wavefunction is composed contains a significant fraction of states that are weakly interacting (aka 'dark eigenstates'), then the measured cross section for that interaction will be much reduced.

### 2.2.2 Dark eigenstates of the eigenspectral ensemble of a large gravity well

The remarkable thing about the eigenspectral ensemble of a large gravitational structure such as a galactic halo is that, in addition to the vast array of states which would normally make up the quantum description of any localised 'visible' particle, it also contains vast numbers of gravitational eigenstates that are weakly interacting or 'dark'. These dark states are the highly excited, high angular momentum (high  $(n,l)$ ) states of Figure 1 (those closest to the left hand curve of the  $(n,l)$  diagram, that is the dotted curve  $p=1$  where we have

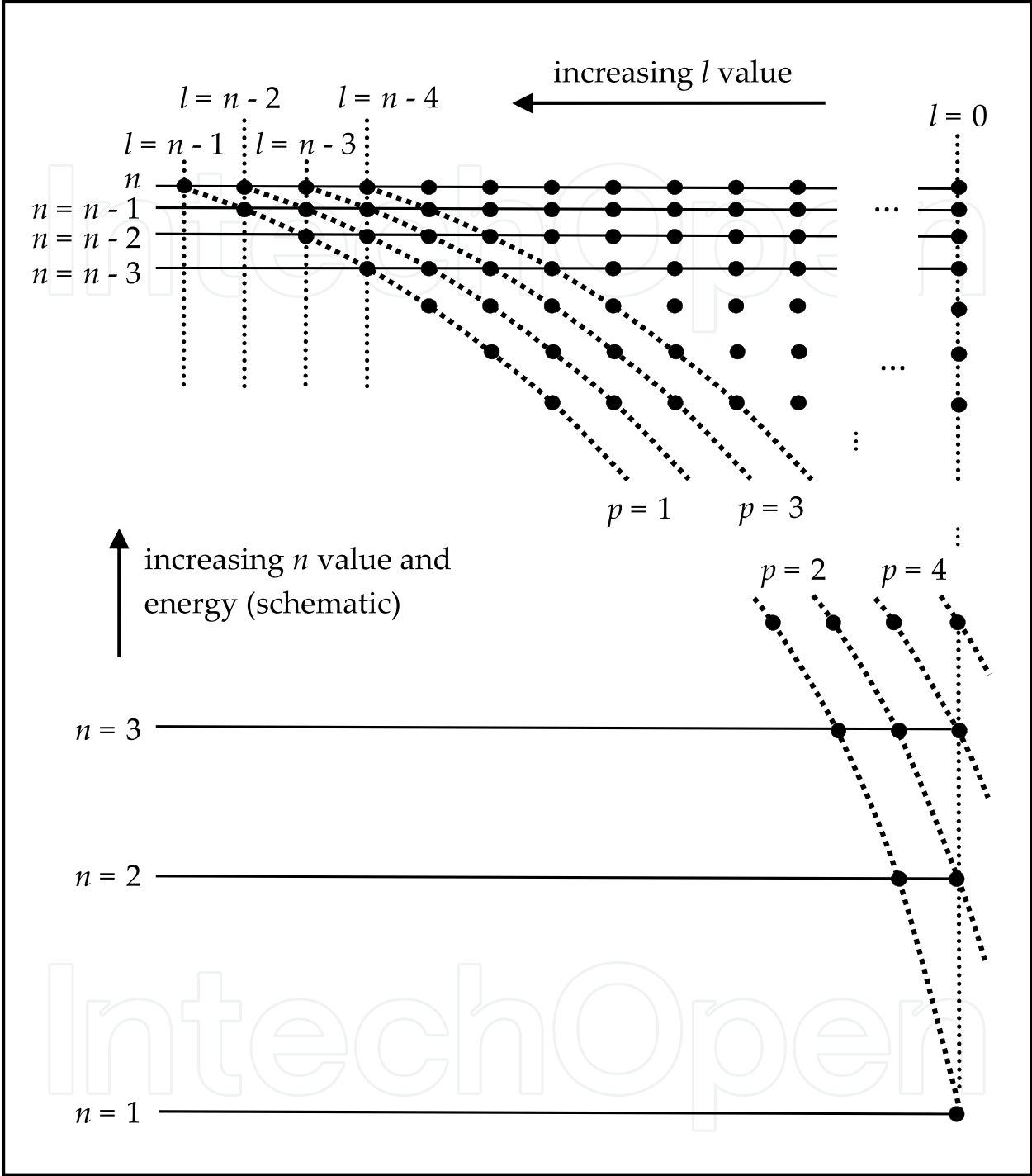


Fig. 1. Schematic  $(n,l)$  diagram showing the high  $n, l, m$ -valued stationary states, drawn to emphasize the values of the parameter  $p = n - l$  (dotted curves). Each solid circle on the diagram represents  $2l + 1$ ,  $z$ -projection ( $m$ -valued) substates.

introduced the notation  $p \equiv n - l$ ) and are somewhat analogous to the Rydberg states in atoms, but have much long lifetimes, extreme stability and are much more robust because of the physical scale of the potential. A wavefunction whose eigenspectral array on the  $(n,l)$  diagram determines it as existing as a relatively localised particle in classical phase space



predisposes it to having similar interaction cross sections to those determined in standard laboratory measurements.

We stress this point in another way: The localisation of a particle in phase space is determined by a wavefunction that not only yields the localisation, but also an average position and momentum in that space. There are however many other eigenspectral distributions that could yield the same average momentum and position in phase space but that would describe particles with very different cross sections. It is possible in principle to form an eigenspectral array with a similar average phase space location as a localised particle, but which is composed predominantly of dark gravitational quantum states. Although particles might possess a similar average momentum and position as their visible counterparts, but they will be weakly acting, invisible and unable to reach equilibrium with visible localised matter via traditional thermalizing interaction processes. Particles with such distributions can form the basis of dark matter.

Predominantly dark gravitational eigenspectral arrays represent an attractive solution for the dark matter problem because (1) they can potentially arise naturally in the universe as a direct prediction of quantum mechanics and (2) they can be used to explain the nature and origin of dark matter without the need for any new physics or new particles. As will be seen later, 'dark-gravitational-eigenstate' dark matter appears to possess properties that fit with many observations of dark matter behaviour, including an inability to gravitationally collapse or coalesce, a transparency to light and other parts of the electromagnetic spectrum, and does not suffer from the same problems associated with other CDM WIMP candidates. Eigenstructure halos formed from vast arrays of particles with predominantly high- $l$ , dark eigenspectra enable the success of LCDM cosmology on large scales to be retained while yielding properties that remove the difficulties faced by LCDM on the galactic cluster/galaxy scale and below.

### 3. Schrödinger-type solutions to gravitational potentials

#### 3.1 Solution of the simple central point potential

More complex arrangements of gravitational binding than that discussed in 2.1 are possible, for example agglomerations of elementary neutral particles bound in a 'collective' gravitational potential well in a similar manner to the structure of nuclear material. We begin here however with the Schrödinger approach to the central point potential and make refinements on this. The analysis for this has been done elsewhere and we give a brief summary here. (For more detail see Ernest, 2009a.) The gravitational form of Schrodinger's equation for a two particle system is written as

$$-\frac{\hbar^2}{2\mu}\nabla^2\psi - \frac{Gm_0M_0}{r}\psi = i\hbar\frac{\partial\psi}{\partial t} \quad (1)$$

where  $M_0$  and  $m_0$  are the masses of the large central and small 'orbit' point particles respectively,  $\mu$  is the reduced mass and the other symbols have their normal meanings. Separation of variables leads to the eigenenergies  $E_n$  and normalised eigenfunctions  $u_{n,l,m}(\mathbf{r},t)$ , which are given by  $E_n = -\mu G^2 m_0^2 M_0^2 / 2\hbar^2 n^2$  and  $u_{n,l,m}(\mathbf{r},t) = R_{n,l}(r)Y_{l,m}(\theta,\phi)$ , where  $n$ ,  $l$  and  $m$  are

the standard quantum numbers.  $Y_{l,m}(\theta, \phi)$  are the spherical harmonics. The limits of the angular eigenfunction components for large  $m$  and  $l$  are not significant for the present discussion and have been dealt with previously (Ernest, 2009a). The radial component  $R_{n,l}(r) = N_{nl}(2r/nb_0)^l \exp(-r/nb_0) L_{n-l-1}^{2l+1}(2r/nb_0)$  is written in terms of Laguerre polynomials

$$L_{n-l-1}^{2l+1}(2r/nb_0) = (n+l)! \sum_{k=0}^{n-l-1} (-1)^{k+2l} (2r/nb_0)^k (n-l-1-k)! (2l+1+k)! k! \quad \text{where}$$

$b_0 = \hbar^2 / G\mu m_0 M_0$  is a scale factor analogous to the atomic case, and  $N_{nl} = (2/nb_0)^{3/2} ((n-l-1)! / 2n(n+l)!)^{1/2}$  is a normalising constant. The radial eigenfunctions are very significant in developing the present theory and we concentrate on these from now on. The states are shown in Figure 1 where, for a central point-mass potential as in this diagram, the set of all  $l$  and  $m$  values is degenerate for any given value of  $n$ .

In Figure 1 the  $l$ - $m$ -degenerate  $n$  levels are shown in proportion schematically to their state energy  $\propto 1/n^2$  but it should be noted that their average radial positions behave in the opposite way: approximately  $\propto n^2$ . For the high- $l$ , high- $n$  states the average radial position is accurately written as  $\langle r_n \rangle = n^2 b_0$ . The radial eigenfunction extent  $r_{\max} - r_{\min}$  spreads out as a square root dependence on the value of  $p$ , approximately centred on  $n^2 b_0$ . The position of the eigenfunctions is important because a sufficient density of occupied states can in principle modify the potential so it is no longer that of a central point-mass. The deviation from a point potential can be approximately allowed for by incorporating  $b_0$  as a variable dependent on the enclosed variable mass  $M(r)$ . Each  $M(r)$  gives an eigenvalue series of energies  $E_{n_1}^{(M_1)}$ ,  $E_{n_2}^{(M_2)}$ ,  $E_{n_3}^{(M_3)}$  ... and the appropriate  $n$  chosen from each series  $\{n_1\}$ ,  $\{n_2\}$ ,  $\{n_3\}$ , ... using the value of  $M(r)$  determined from its functional form. This method works but it is not the optimal approach.

### 3.2 Solutions for halo mass distributions and logarithmic potentials

Solutions to the gravitational central-point-potential Schrodinger equation given above can be shown to contain some states that possess the fundamental properties required for dark matter. The galaxy and clusters however are not point potentials but have extended mass distributions. As mentioned earlier, the radial velocity profiles of galaxies for example show constant velocities with radius as far out as can be measured rather than the expected Keplerian decline. This implies a radial density profile that varies as  $1/r^2$ . The force is then proportional to the enclosed mass  $M_{\text{enclosed}}$  which is therefore given by

$$F = \frac{Gm_0 M_{\text{enclosed}}}{r^2} = \frac{Gm_0}{r^2} \int_0^r \rho(r') 4\pi r'^2 dr' = \frac{Gm_0}{r^2} \int_0^r \frac{k}{r'^2} 4\pi r'^2 dr' = \frac{Gm_0 M_0}{R_0 r}$$

where  $k = M_0 / R_0$  is the density proportion constant and  $R_0$  is the hypothetical radius of the halo whose total mass out to  $R_0$  is now  $M_0$ . Since  $F = -\nabla V$  we have that

$$V(r) = -\int_{\infty}^{R_0} -GM_0 / r^2 dr - \int_{R_0}^r -GM_0 / R_0 r dr \quad \text{and}$$

$$\begin{aligned}
 V(r) &= -\frac{Gm_0M_0}{r} & (r \geq R_0) \\
 &= -\frac{Gm_0M_0}{R_0} \ln\left(\frac{R_0 e}{r}\right) & (r < R_0)
 \end{aligned} \tag{2}$$

where again  $m_0$  is the 'orbit mass and  $e$  the natural logarithm base. This hybrid  $1/r$ -logarithmic potential differs from the equivalent point-mass,  $1/r$  point potential substantially at low  $r$  although in principle the characteristics of the high- $l$ ,  $n$  quantum states of  $1/r$  potentials that make them suitable as fundamental components of dark matter eigenspectral arrays will have equivalent states in the eigenstate ensembles of the real logarithmic halo potentials. In the central point-mass potential case it was possible (Ernest 2009a, 2009b) to obtain approximations for the energies and wavefunction forms of the eigenstates which can be used to obtain quantitative values for interaction rates etc. It is clearly important to be able to develop approximations for similar states in the real logarithmic potentials of the galactic halo case which we now do below.

For wavefunctions inside the halo, the logarithmic potential Schrödinger equation becomes

$$-\frac{\hbar^2}{2\mu} \nabla^2 \psi - \frac{Gm_0M_0}{R_0} \ln\left(\frac{R_0}{r}\right) \psi = i\hbar \frac{\partial \psi}{\partial t} \tag{3}$$

which, on separation of variables, gives the equation for the radial component  $u_{n,l}(r)$  of the wavefunction as

$$-\frac{\hbar^2}{2\mu} \frac{\partial^2 u_{n,l}(r)}{\partial r^2} - \left( \frac{Gm_0M_0}{R_0} \ln\left(\frac{R_0}{r}\right) - E_{n,l} \right) u_{n,l}(r) = 0 \tag{4}$$

The Schrödinger equation is known to be analytically solvable for  $1/r$  and  $-r^2$  potentials but equations with logarithmic potentials require approximation techniques. The equation can be recast into a standard form as

$$-\frac{\hbar^2}{2m_0} \frac{d^2 u_{n,l}(r)}{dr^2} + \left( -\frac{Gm_0M_0}{R_0} \ln\left(\frac{R_0 e}{r}\right) + \frac{\hbar^2 l(l+1)}{2m_0 r^2} - E_{n,l} \right) u_{n,l}(r) = 0 \tag{5}$$

where  $l$  is the angular momentum quantum number. A few attempts have been made to solve this equation. Ciftci et al. (2003) developed approximate solutions for various power-law and logarithmic potentials based on extensions of the Laguerre solutions applicable to  $1/r$  potentials. Their procedure however, when applied to the present case, involves summations (over  $n$ ) with prohibitively large numbers of terms of Laguerre polynomial coefficients.

The technique used here involves first finding the eigenenergies of the states that correspond to the highest angular momentum for any given  $n$  value, that is, all the states that have  $p=1$  (i.e.  $l=n-1$ ) for each  $n$ . These eigenstates have a thin single peaked radial form. For  $m=m_{\max}=\pm l$  the states are ring-like or circular. The energy may be deduced semi-classically noting that all the probability density lies at essentially the same radius  $r_n$ , giving the state 'potential' energy as  $E_U(r_n) \approx -GM_0m_0 / R_0 \ln(R_0 e / r_n)$ . The number of polar

oscillations is  $l_{\max} \approx n$ , giving  $\lambda \approx 2\pi r_n/n$ , and momentum  $m_0 v = \hbar n/r_n$  using the de Broglie relation. The equivalent “kinetic” energy is then  $E_K \approx Gm_0 M_0/2R_0$  and the net energy of the state is therefore

$$E_{n,p=1}(r_n) = E_{n,l=n-1}(r_n) \approx -\frac{Gm_0 M_0}{R_0} \ln\left(\frac{R_0 \sqrt{e}}{r_n}\right) \quad (6)$$

As the quantum number  $m$  decreases, the state form spreads gradually in the  $\pm$  polar direction yielding thin annular shells, ultimately creating a closed spherical shell for  $m=0$ . These states simply represent variations in the polar-azimuthal orientation and so (6) corresponds to the energy of all  $m$  sublevels of the  $l$  value. The energy of the lower  $m$ -states is the same as for the maximum value of  $m$ , both by symmetry and because classically lower  $m$ -values behave simply as mixtures of tilted circular states of equivalent energy.

For the circular states the velocity  $v$  can also be written as a (halo-constant)  $v = \sqrt{GM_0/R_0}$ , by equating the centripetal and gravitational force based on the enclosed mass. Combined with  $m_0 v = \hbar n/r_n$ , this allows  $r_n$  to be expressed in terms of  $n$  and leads to an expression for the energy level levels  $E_{n,p=1}$  for the circular ( $p=1$ ) states (compared with  $E_{n, \text{all } p} = -\mu G^2 m_0^2 M^2 / 2\hbar^2 n^2$  in the centralised point-mass case).  $r_n$  and  $E_{n,p=1}$  are given by

$$r_n = n\hbar \sqrt{\frac{R_0}{Gm_0^2 M_0}} \quad (7)$$

$$E_{n,p=1}(r_n) = E_{n,l=n-1}(r_n) \approx -\frac{Gm_0 M_0}{2R_0} \ln\left(\frac{Gm_0^2 M_0 R_0 e}{n^2 \hbar^2}\right)$$

where the  $E_{n,l}$  are the energy eigenvalues which will in general depend on both  $n$  and  $l$ .

Each of these states is itself the lowest energy eigenvalue in a set of eigenvalues all of which have the same value of  $l$ , say  $l=l'$  and increasing values of  $n$  and  $p$ , that is  $p=1, 2, 3 \dots$ . The energies are  $E_1 = E_{n=l'+1, l=l', p=1}$ ,  $E_2 = E_{n=l'+2, l=l', p=2}$ ,  $E_3 = E_{n=l'+3, l=l', p=3} \dots$  with  $E_1$  given by equation (7).

The quantity  $\hbar^2 l(l+1)/2mr^2$  in equation (5) may be thought of as the ‘centrifugal potential’ and for each value of  $l$  we define the effective potential energy as

$$V_{\text{effective}}(r, l) = -\frac{Gm_0 M_0}{R_0} \ln\left(\frac{R_0 e}{r}\right) + \frac{\hbar^2 l(l+1)}{2m_0 r^2}, \quad r \leq R_0$$

$$V_{\text{effective}}(r, l) = -\frac{Gm_0 M_0}{r} + \frac{\hbar^2 l(l+1)}{2m_0 r^2}, \quad r > R_0 \quad (8)$$

plots of which are shown in Figure 2.

The maximum energy depths  $E_d$  of the well minima and their corresponding radial positions are given by

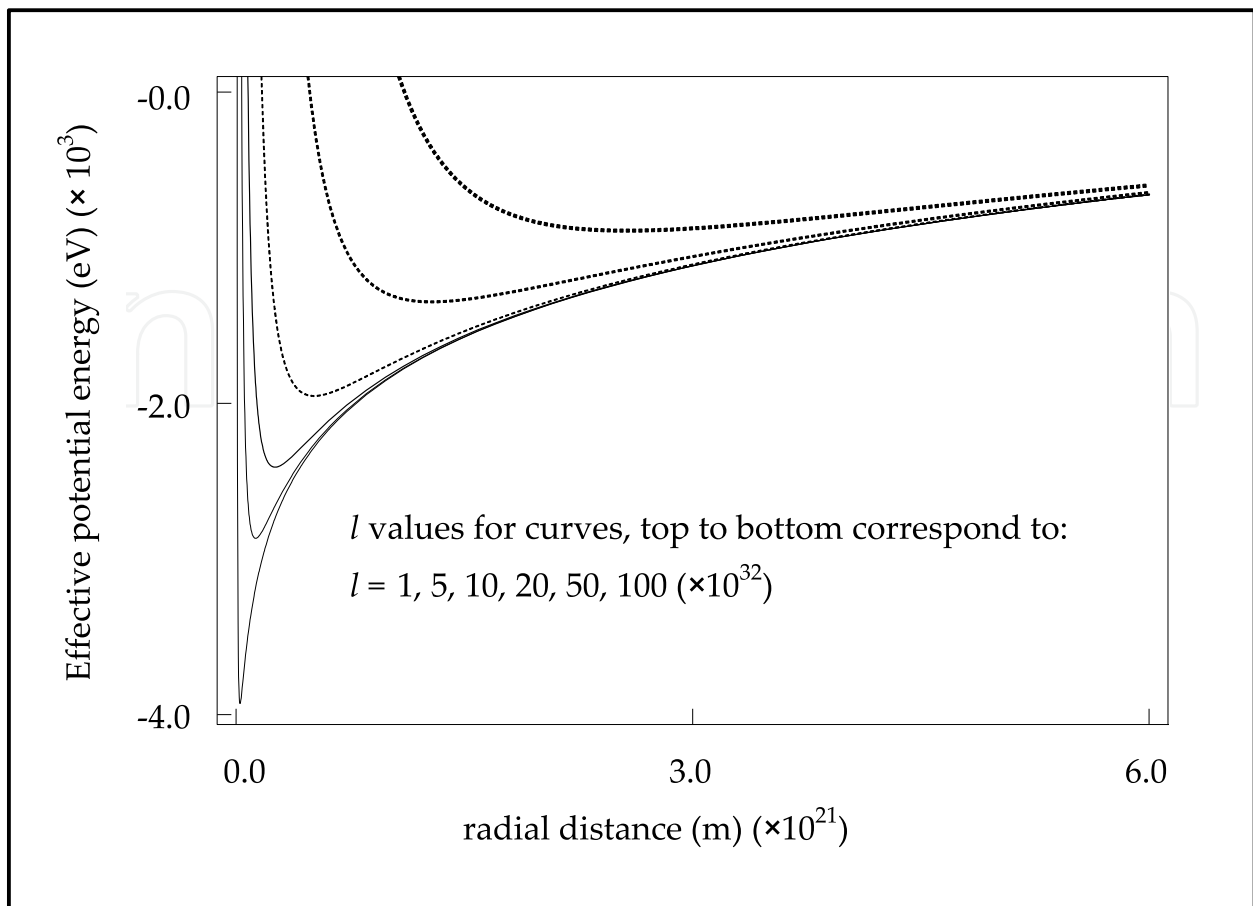


Fig. 2. Effective halo potentials for various  $l$ .  $M_0 = 6.0 \times 10^{42}$  kg,  $m_0 = 1.6 \times 10^{-27}$  kg,  $R_0 = 3.0 \times 10^{21}$  m; curves, top to bottom, correspond to  $l = 1, 5, 10, 20, 50, 100$  ( $\times 10^{32}$ )

$$E_d = -\frac{Gm_0M_0}{2R_0} \ln \left( \frac{Gm_0^2M_0R_0e}{l(l+1)\hbar^2} \right) \quad (9)$$

and

$$r_d = \sqrt{\frac{l(l+1)R_0\hbar^2}{Gm_0^2M_0}} \quad (10)$$

Within each well (characterised by its  $l$ -value) the lowest the energy state (labelled say by  $\nu=0$ ) is a  $p=1$  eigenstate and corresponds to the  $n$ -value  $n=l+1$ . For  $n$  states not too much greater than  $l$  we use a simple harmonic Taylor series approximation around the minimum, which is analytically solvable to obtain a set of energy eigenvalues and eigenfunctions for any  $n > l+1$  provided  $n$  is not too far above  $l$ . (For typical galactic halo parameters the harmonic approximation gives better than 1% accuracy to the potential over the region of the well encompassed by eigenstates with  $p$  from 1 to  $10^{20}$  - see Figure 3).

The harmonic form of the Schrödinger equation is

$$-\frac{\hbar^2}{2m_0} \frac{d^2u_\nu(r)}{dr^2} + \frac{1}{2}m_0\omega^2r^2u_\nu(r) - E_\nu u_\nu(r) = 0 \quad (11)$$



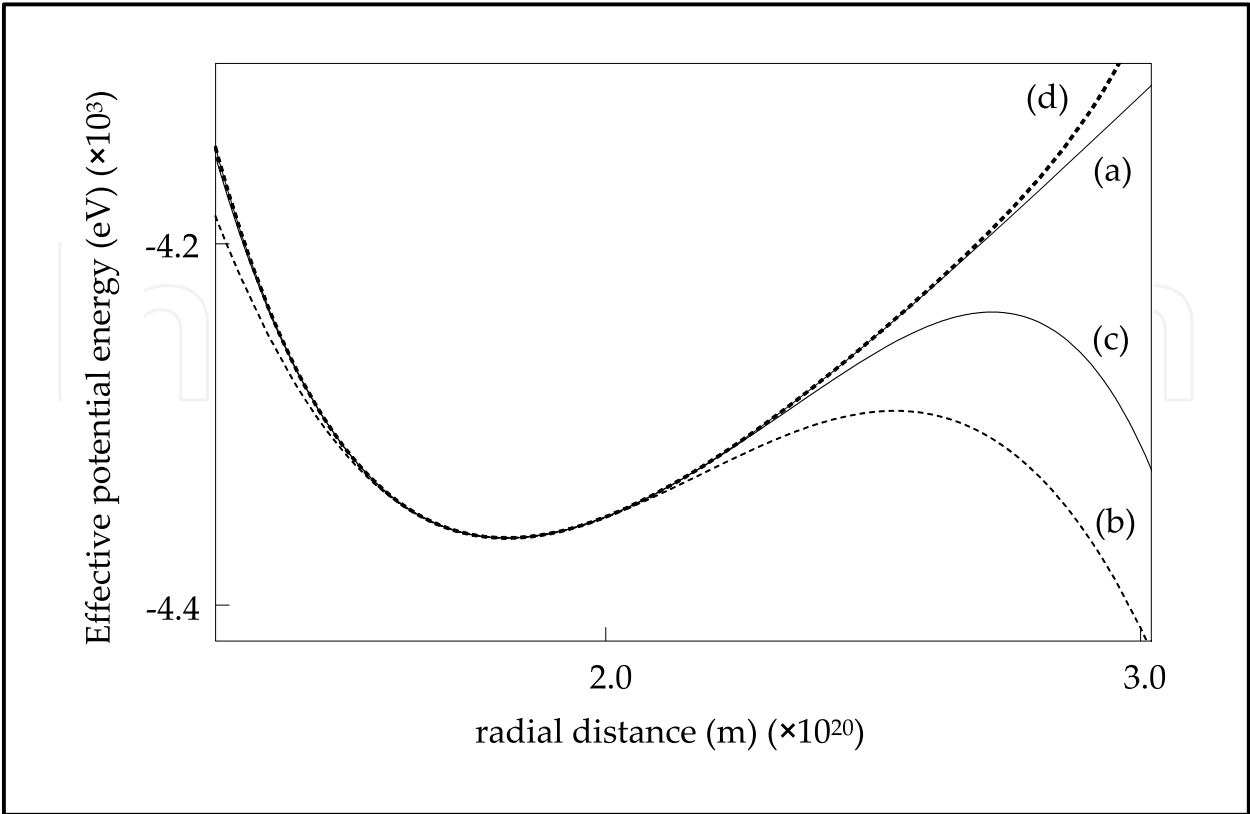


Fig. 3. Taylor approximations to the  $l = 3.0 \times 10^{33}$  effective halo potential.  $M_0 = 6.0 \times 10^{42}$  kg,  $m_0 = 1.6 \times 10^{-27}$  kg,  $R_0 = 3.0 \times 10^{21}$  m, Curve: (a) exact potential, (b) 3 term approximation (harmonic potential), (c) 5 term approximation, (d) 10 term approximation.

and putting  $r' = r - r_d$  leads to an equation of the form of equation (11) equivalent to (5) as

$$\begin{aligned} &-\frac{\hbar^2}{2m_0} \frac{d^2 y_v(r')}{dr'^2} + \left( -\frac{Gm_0 M_0}{2R_0 r_d^2} + \frac{3l(l+1)\hbar^2}{2m_0 r_d^4} \right) r'^2 y_v(r') \\ &- \left( \frac{Gm_0 M_0}{R_0} \ln \left( \frac{eR_0}{r_d} \right) - \frac{l(l+1)\hbar^2}{2m_0 r_d^2} + E_n \right) y_v(r') = 0 \end{aligned} \tag{12}$$

provided that

$$\omega = \sqrt{-\frac{GM_0}{R_0 r_d^2} + \frac{3l(l+1)\hbar^2}{m_0^2 r_d^4}} = \frac{Gm_0 M_0}{R_0 \hbar} \sqrt{\frac{2}{l(l+1)}} \tag{13}$$

and

$$E_n = E_v + \frac{l(l+1)\hbar^2}{2m_0 r_d^2} - \frac{Gm_0 M_0}{R_0} \ln \left( \frac{eR_0}{r_d} \right) = E_v - \frac{Gm_0 M_0}{2R_0} \ln \left( \frac{Gm_0^2 M_0 R_0 e}{l(l+1)\hbar^2} \right) \tag{14}$$

The eigenvalue and eigenfunction solutions to (11) are those for the standard harmonic oscillator, given by

$$\begin{aligned}
 E_\nu &= \left( \nu + \frac{1}{2} \right) \hbar \omega, \quad \nu = 0, 1, 2, \dots \\
 u_\nu(r) &= \left( \frac{m_0 \omega}{\pi \hbar} \right)^{1/4} \frac{1}{\sqrt{2^\nu \nu!}} H_\nu(\xi) \exp(-\xi^2/2)
 \end{aligned}
 \tag{15}$$

where  $H_\nu(\xi)$  are the Hermite polynomials and  $\xi = (r - r_d) \sqrt{m_0 \omega / \hbar}$ . Combining equations (14) and (15), noting that  $\nu$  is related directly to the  $p$ -value for the state by  $\nu = p - 1 = n - l - 1$  and taking care to distinguish between quantum parameters that refer to the well compared to the states within that well, we can write a general formula for the eigenvalues of any high angular momentum (low- $p$ ) state of a logarithmic centrifugal well in terms of the quantum numbers  $n$  and  $l$  as

$$E_{n,l} = \left( \frac{G m_0 M_0}{2 R_0} \right) \left( \frac{\sqrt{2}(2n - 2l - 1)}{\sqrt{l(l+1)}} - \ln \left( \frac{G m_0^2 M_0 R_0 e}{l(l+1) \hbar^2} \right) \right)
 \tag{16}$$

A schematic state diagram similar to that for the central point-mass state ensemble is shown in Figure 4, with a superimposed schematic for the harmonic approximation to the centrifugal well for an angular momentum quantum number  $l$ . The levels ( $\nu = 0, 1, 2 \dots$ ) of the centrifugal well schematic correspond to the increasing values of  $p$  and  $n$  and constant  $l$ , beginning with the state  $n = l + 1$ ,  $p = 1$ . The lines of constant- $n$  are no longer horizontal because of the additional dependence of the energy on  $l$ . It is of interest to compare the energy level differences between two adjacent  $l$ -values with two adjacent  $n$ -values since this gives a measure of the degree to which the presence of a logarithmic potential affects the otherwise degenerate  $l$ -states of the classic central point-mass potential. Equation (16) shows that for any given  $l$ , the state energy increases linearly with  $n$  as anticipated from the discussion of the circular states discussed earlier in this section. Indeed as  $l$  approaches  $n$ , equation (16) approaches equation (7), as expected. Putting  $l \approx \sqrt{l(l+1)}$  and noting that  $l$  is close to  $n$ , partial differentiation of equation (16) with respect to  $n$  and  $l$  gives the energy spacing per unit change in  $n$  and  $l$  as:  $\partial E_{n,l} / \partial n \approx \sqrt{2} G m_0 M_0 / l R_0$  and  $\partial E_{n,l} / \partial l \approx -G m_0 M_0 (\sqrt{2} n - l) / l^2 R_0$  respectively. For  $l \sim n$ ,  $(\sqrt{2} n - l) \sim (\sqrt{2} - 1) l$ , hence  $\partial E_{n,l} / \partial l \approx \partial E_{n,l} / \partial n \times (\sqrt{2} - 1) / \sqrt{2} \approx 0.3 \partial E_{n,l} / \partial n$  so that the energy spacing for adjacent  $l$ -states in the extended  $1/r^2$  density distribution is a substantial fraction of the energy spacing of adjacent  $n$ -states, as illustrated in Figure 4, and in contrast to the angular momentum degeneracy observed for the eigenstates in the central point-potential. Also since  $\partial E_{n,l} / \partial l$  is always negative, state energy increases as  $l$  decreases (at least for the  $\sim 10^{20}$   $p$ -values that are within the range of validity of the harmonic approximation) so that the low angular momentum states are less well bound than the high angular momentum ones for any given  $n$ . For the typical halo parameters  $M_0 / R_0 = 2.0 \times 10^{21}$  kg/m,  $m_0 = 1.67 \times 10^{-27}$  kg, and taking  $r = 1.0 \times 10^{21}$  m ( $l \sim 6 \times 10^{33}$ ) as a typical outer halo position, the energy spacing for adjacent  $n$  states is  $\sim 4.8 \times 10^{-32}$  eV, and for  $l$  states is  $\sim 1.6 \times 10^{-32}$  eV. If the same procedure used here is applied to a standard central point-mass potential then the spacing between the harmonic

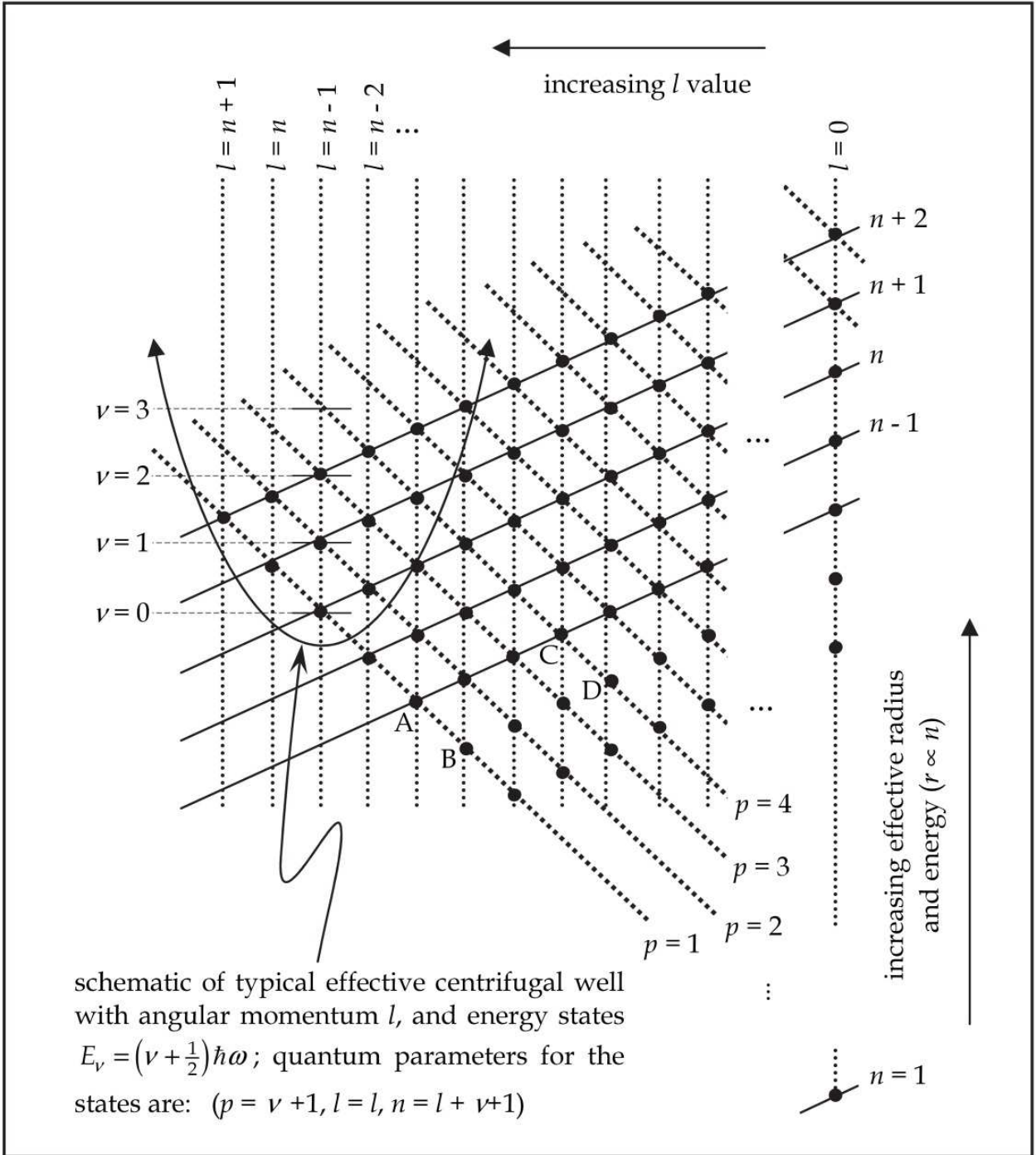


Fig. 4. Schematic  $(n,l)$  state diagram for the logarithmic potential (radial mass density  $\propto 1/r^2$ ) showing the high  $n, l$ -valued stationary states. A typical effective centrifugal  $l$ -well of momentum  $\sqrt{l(l+1)}\hbar$  is shown superimposed on the state diagram to illustrate how the higher energy states  $E_\nu = (\nu + 1/2)\hbar\omega, \nu = 0,1,2\dots$  corresponding to  $(p = \nu + 1, l = l, n = l + \nu + 1)$  are calculated for each  $l$ -well. Each solid circle on the diagram represents  $2l + 1, z$ -projection ( $m$ ) substates.

levels gives essentially the same result as that obtained directly from equation (1) which is again a check on the validity of the approach. That is the energy of a particular vibrational level in one  $l$ -harmonic well becomes equal to the energy of one level above or below in the adjacent,  $l \pm 1$  well, making the energy levels for different  $l$ , same  $n$  degenerate as expected.

It is also possible to write down the eigenfunctions of the high angular momentum eigenstates in a logarithmic potential. It is necessary to generalise the normalisation constant  $(m_0\omega/\pi\hbar)^{1/4}/\sqrt{2^\nu\nu!}$  in equation (15). Writing the second of equations (15) as  $u_\nu(r) = N H_\nu(\xi) \exp(-\xi^2/2)$  where  $N = (m_0\omega/\pi\hbar)^{1/4}/\sqrt{2^\nu\nu!}$ , and  $\xi = \alpha r - \beta$ , where  $\alpha = (2l(l+1))^{1/4}/r_d$  and  $\beta = (2l(l+1))^{1/4}$ , we modify the procedure of Schiff (1968) to find  $N$ . The integral for calculating the normalising constant is given by

$$\begin{aligned} N^2 \int_0^\infty |u_\nu(\alpha r - \beta)|^2 r^2 dr &= 1 \\ \frac{N^2}{\alpha^3} \int_0^\infty |u_\nu(\alpha r - \beta)|^2 (\alpha r)^2 d(\alpha r) &= 1 \end{aligned} \quad (17)$$

Now  $\alpha r \gg 1$  and is approximately constant and equal to  $\alpha r_d$  over the significant range of the integrand and it can therefore be taken outside the integral to give

$$\frac{N^2 r_d^2}{\alpha} \int_0^\infty |u_\nu(\alpha r - \beta)|^2 dr = 1 \quad (18)$$

Furthermore the integral  $\int_{-\infty}^\infty |u_\nu(\alpha r)|^2 d(\alpha r)$  is essentially the same as  $\int_0^\infty |u_\nu(\alpha r - \beta)|^2 dr$  since it is merely a displacement of the harmonic function from  $r=0$  to  $r=r_d$  so (17) may be written as

$$\frac{N^2 r_d^2}{\alpha} \int_{-\infty}^\infty H_\nu(\alpha r)^2 \exp(-(\alpha r)^2) = 1 \quad (19)$$

Using the Hermite generating function relation  $e^{-s^2+2s\alpha r} = \sum_{i=0}^\infty H_\nu(\alpha r) s^i / i!$ , expanding the exponential as a power series and equating series coefficients, enables the integral in equation (18) as  $\pi^{1/2} 2^\nu \nu!$  (see Schiff, 1968 for details) and gives the normalising constant  $N$  as

$$N = \frac{1}{r_d} \left( \frac{\alpha}{\sqrt{\pi} 2^\nu \nu!} \right)^{1/2} = \left( \frac{(2l(l+1))^{1/4}}{r_d^3 \sqrt{\pi} 2^\nu \nu!} \right)^{1/2} \quad (20)$$

Thus the eigenfunctions  $u_{l,p}(r)$  (or  $u_{n,l}(r)$ ) may be written in terms of the well parameters  $r_d$  and  $l$ , as

$$\begin{aligned}
 u_{l,p}(r) &= \left( \frac{(2l(l+1))^{1/4}}{r_d^3 \sqrt{\pi} 2^{p-1} (p-1)!} \right)^{1/2} \times \\
 &\quad H_{p-1} \left( (2l(l+1))^{1/4} \left( \frac{r}{r_d} - 1 \right) \right) \exp \left( -\frac{(l(l+1))^{1/2}}{\sqrt{2}} \left( \frac{r}{r_d} - 1 \right)^2 \right) \\
 u_{n,l}(r) &= \left( \frac{(2l(l+1))^{1/4}}{r_d^3 \sqrt{\pi} 2^{n-l-1} (n-l-1)!} \right)^{1/2} \times \\
 &\quad H_{n-l-1} \left( (2l(l+1))^{1/4} \left( \frac{r}{r_d} - 1 \right) \right) \exp \left( -\frac{(l(l+1))^{1/2}}{\sqrt{2}} \left( \frac{r}{r_d} - 1 \right)^2 \right)
 \end{aligned} \tag{21}$$

where  $r_d$  is defined as in equation (10).

#### 4. High angular momentum states: Longevity, darkness, transparency, stability and weak interaction with low l-states

High angular momentum, high- $n$  gravitational eigenstates make excellent dark matter candidates. Any particle, even traditional baryons or electrons, placed into these states or into wavefunctions whose eigenspectral composition is rich in high- $n, l$  states will be dark, weakly interacting and unable to gravitationally collapse in the traditional classical sense. Why is this?

Quantum theory provides standard ways to calculate the interaction properties of eigenstates such as spontaneous and stimulated emission and absorption rates, particle interaction cross-sections etc. These rates depend, among other things, on the overlap integral (matrix element) for the interaction, which itself depends on the initial and final states and on the interaction Hamiltonian, generally expressed as a combination of spatial and momentum (differential) operators. In the case of radiative dipole decay for example the rate  $A_{i,f}$  is given by (Ernest, 2009b):

$$A_{i,f} = \frac{\omega_{if}^3 |\langle f | e \mathbf{r} | i \rangle|^2}{3 \varepsilon_0 \pi \hbar c^3} = \frac{\omega_{if}^3 \Pi_{if}^2}{3 \varepsilon_0 \pi \hbar c^3} \tag{22}$$

where  $e$  is the electronic charge, the  $\varepsilon_0$  electrical permittivity,  $|\langle f | e \mathbf{r} | i \rangle| = \Pi_{if}$  the absolute value of the dipole matrix element for spontaneous decay for the transition  $i$  to  $f$ ,  $\omega_{if}$  the transition angular frequency, and the other symbols have their usual meanings.  $|\langle f | e \mathbf{r} | i \rangle| = \Pi_{if}$  is given (Ernest, 2009b) as normal by

$$\begin{aligned}
 \Pi_{if} &= \left| \int_0^\infty \int_0^\pi \int_0^{2\pi} R_{nf,lf}^* Y_{lf,mf}^* e \mathbf{r} R_{ni,li} Y_{li,mi} r^2 \sin^2(\theta) \cos(\phi) d\phi d\theta dr \right| \\
 &= \sqrt{(\Pi_{ifx}^2 + \Pi_{ify}^2 + \Pi_{ifz}^2)}
 \end{aligned} \tag{23}$$



where  $\Pi_{ifx}, \Pi_{ify}$  and  $\Pi_{ifz}$  are standard Cartesian components, expressible in terms of angular and radial overlap integrals  $I_{\theta,\phi,x}, I_{\theta,\phi,y}, I_{\theta,\phi,z}, I_r$  over the initial,  $i$ , and final,  $f$ , spherical harmonic  $Y_{m,l}(\theta, \phi)$  and radial component  $u_{n,l}(r)$  eigenfunctions:

$$\begin{aligned} I_{\theta\phi x} &= \int_0^\pi \int_0^{2\pi} Y_{lf,mf}^* Y_{li,mi} \sin^2(\theta) \cos(\phi) d\phi d\theta \\ I_{\theta\phi y} &= \int_0^\pi \int_0^{2\pi} Y_{lf,mf}^* Y_{li,mi} \sin^2(\theta) \sin(\phi) d\phi d\theta \\ I_{\theta\phi z} &= \int_0^\pi \int_0^{2\pi} Y_{lf,mf}^* Y_{li,mi} \cos(\theta) \sin(\theta) d\phi d\theta \\ I_r &= \int_0^\infty u_{nf,lf}^*(r) r^3 u_{ni,li}(r) dr \end{aligned} \quad (24)$$

Ernest (2009b) calculated state to state dipole decay times  $1/A_{i,f}$  based on a central point-mass potential. Using the logarithmic potential developed here, decay times remain very similar. Times are affected by the choice of the density parameter  $M_0/R_0$  but if the same enclosed mass is used the energy spacing between levels is only marginally different. For example the differences in energy spacing (occurring as a result of differences in the shape of the well for the two different potentials) between two adjacent  $p=1$  states with  $\Delta p=0$  (such as  $A \rightarrow B$  on Figure 4) for logarithmic (real halo) versus point-mass potentials produce differences in decay times of less than 5% for the same enclosed mass at typical galactic halo radii. As a result particles occupying these states (or predominant mixtures of them) in the logarithmic potentials corresponding to actual galactic halos do not emit radiation, are stable over cosmic lifetimes and do not undergo gravitational collapse. We restate this important result:

- The lifetimes of the high angular momentum states are far greater than the age of the universe and the states are stable and do not emit radiation.

Similar arguments apply to  $\Delta p=0$  transitions originating on the 'deeper'  $p=2,3,4\dots$  states (such as  $C \rightarrow D$  on Figure 4), provided that  $p$  is a negligible fraction of  $n$ . These lifetimes remain long even when the number of available decay channels is taken into account (selection rules require that  $\Delta l = \pm 1$  and  $\Delta m = 0, \pm 1$ ). This was discussed extensively by Ernest (2009b) and is related to the effects that eigenfunction orthogonality, large radial position and differences in spatial oscillation frequency (SOF) have on the overlap integral. (Where transitions are involved that 'cross' lines of constant  $p$  on the state diagram, it can be shown (Ernest, 2009b) that the overlap integrals become exceedingly small.) We do not repeat the arguments in detail here but note that the results can be applied in the same way with essentially the same conclusions to the states of the logarithmic potential wells.

The extreme longevity of the low- $p$  states has implications for the rates of stimulated emission and absorption. The probability per unit time  $P_{if}$  of stimulated emission or absorption of radiation from a state  $i$  to a state  $f$  is given by

$$P_{if} = \frac{\pi e^2}{3\epsilon_0 \hbar^2} |\langle f | \mathbf{r} | i \rangle|^2 \rho(\omega_{if}) = \frac{\pi \Pi_{if}^2}{3\epsilon_0 \hbar^2} \rho(\omega_{if}) = \frac{4\pi^2 \Pi_{if}^2}{3\epsilon_0 \hbar^2 c} I(\omega_{if}) \quad (25)$$

where  $\rho(\omega_{if})$  is the radiation energy density per unit angular frequency and  $I(\omega_{if})$  is the corresponding beam intensity per unit angular frequency. Assuming the upper and lower degeneracies are similar one can calculate the absorption and scattering times for photons as they pass through a typical halo. The details of this calculation are derived explicitly in Ernest (2009b). The calculation derived there shows that photons in virtually all known regions of the electromagnetic spectrum will pass through the halo without scattering via low- $p$  eigenstates, so that halos composed of such states will be completely transparent and not subject to the usual processes of Compton or Raleigh scattering as are traditional localised 'free' particles represented by visible eigenspectral ensembles. Again these calculations extend immediately to the eigenstates of the logarithmic potentials with essentially the same results. We therefore also explicitly note that:

- A halo consisting of ordinary particles composed predominantly of low- $p$  eigenspectral components will be transparent to virtually all regions of the electromagnetic spectrum.

Interactions of low- $p$  eigenstates with other particles involve different Hamiltonian operators and are not subject to the same stringent selection rules as with photon interactions, particularly for three body 'collisions'. We therefore expect that low- $p$  eigenstates will not be as 'dark' for particles as they are for photons. It turns out however that it is still difficult for state transfer across lines of constant  $p$ , particularly when  $p$  is small. The reasons behind this relate to several properties of the low- $p$  states. These include their limited radial range, the limited number of, and wavelength of, their spatial oscillations, and the effect of differences in the SOF between the initial and final quantum states. These aspects were discussed by Ernest (2009b). It was seen in figure 9 of that paper that there is a relationship between the relative spatial oscillation frequency (RSOF) of the initial and final states and the size of the overlap integral. If one state has  $p=1$  then the value of  $\log(-\log(I_r))$  is linearly related to  $\log(\text{RSOF})$ . Recent work has shown that a similar relationship exists for  $p=2$  states and should hold in general provided  $p$  is a negligible fraction of  $n$ . This relationship means that if either of the states has a low- $p$  value, the size of the overlap integral diminishes rapidly with any difference in  $p$ -values, that is the degree of 'p-crossing'. Furthermore because the interaction Hamiltonian does not have a significant effect on the spatial oscillation frequencies of the states, it means that similar relationships should exist for other types of interactions such as those involving particles. This is a direct consequence of the orthogonality and limited radial extent of the low- $p$  eigenstates.

Figure 5 shows a general summary of the different ways in which 'visible' matter (that is photons and traditional particles in thermalized, broad-range mixtures of halo eigenstates) with low- $p$  states is limited by effects such as spatial oscillation frequency and spatial overlap. In case (a) we have small changes in both  $p$  and  $n$ , and transitions are possible, but the size of the change is so small that changes in energy or momentum of the perturbing entity, and state dispersion effects over cosmic history, are negligible. In case (b) again the change in  $p$  is small, i.e. no significant 'p-crossing' and the initial and final spatial oscillation frequencies are similar ( $\text{RSOF} \sim 1$ ). Transitions are also theoretically possible in this case but here  $\Delta n$  is made large enough to enable observable changes in the momentum and/or energy of the perturbing entity. However exclusively in the low- $p$  regime, the  $\Delta n$  required for such measurable angular momentum or energy changes requires eigenstate functions that are spatially distinct making  $I_r \approx 0$  irrespective of the Hamiltonian involved. In case (c) the initial and final states are no longer spatially distinct (i.e. forced to overlap by

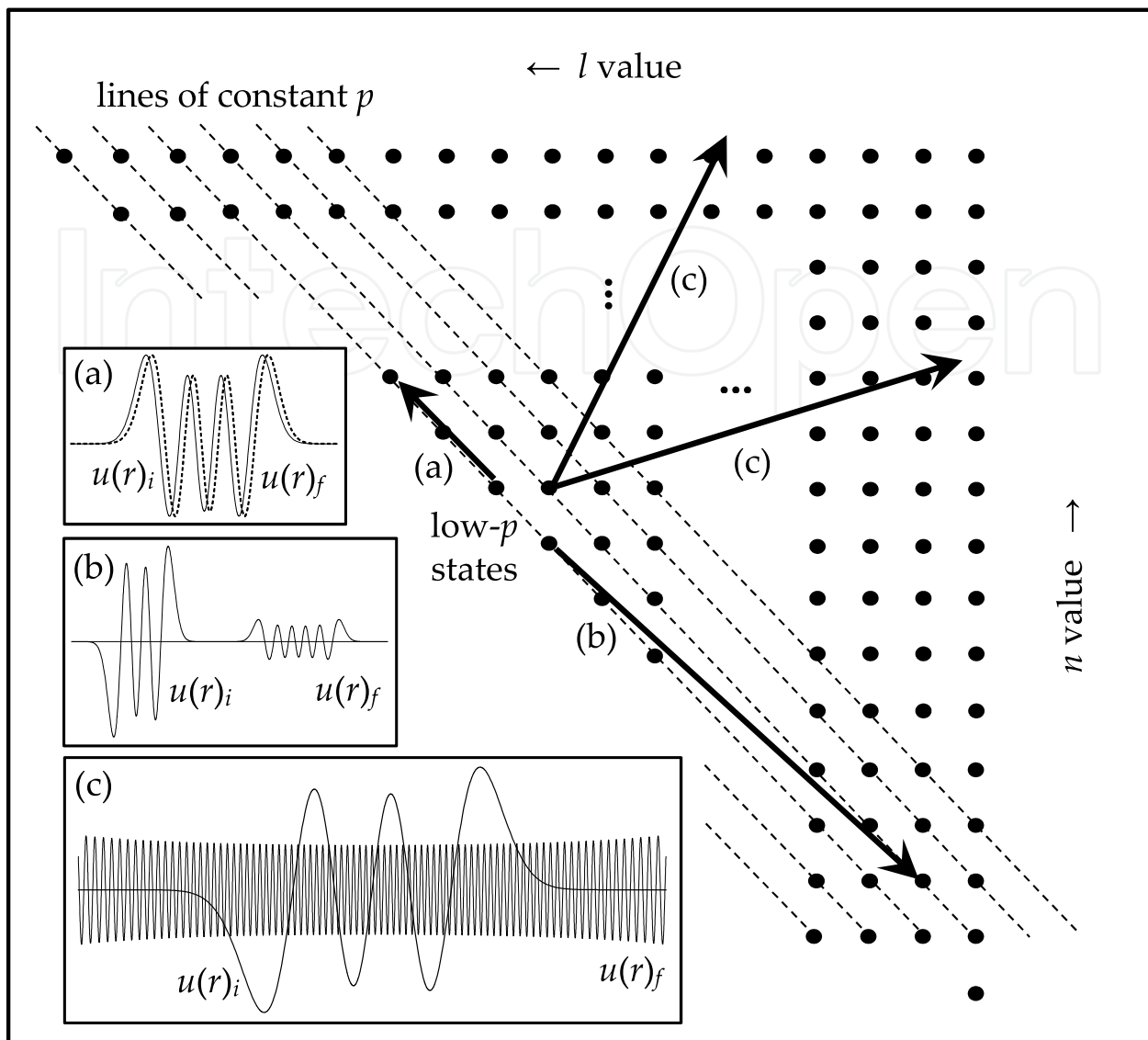


Fig. 5. Schematic  $(n, l)$  state diagram showing how characteristics of low- $p$  initial  $(u(r)_i)$  states, and final  $(u(r)_f)$  states lead to weak interaction:

- case (a) small change in  $p \Rightarrow$  similar SOF; transitions possible,  $I_R \neq 0$  but  $\Delta E, \Delta(mv) \sim 0$
- case (b) small change in  $p \Rightarrow$  similar SOF;  $\Delta n, \Delta l \gg 1 \Rightarrow \Delta E, \Delta(mv) \gg 0$ , but initial final states spatially distinct  $\Rightarrow I_r \sim 0$
- case (c) large change in  $p \Rightarrow$  large differences in SOF;  $\Delta n, \Delta l \gg 1 \Rightarrow \Delta E, \Delta(mv) \gg 0$ , but large relative SOF  $\Rightarrow I_r \sim 0$

the choice of the final state) but still maintain large differences in  $\Delta l$  and  $\Delta n$ . This however requires significant ' $p$ -crossing' and, in a similar way to figure 9 of Ernest (2009b), we expect the resulting differences in spatial oscillation frequency to result in  $I_R \approx 0$ , irrespective of the interaction Hamiltonian involved. Again we note that:

- A halo consisting of ordinary particles composed predominantly of low- $p$  eigenspectral components will be weakly interacting with particles and therefore have difficulty in thermalising and hence redistributing its eigenspectral distribution to that of traditional localised, Maxwellian eigenspectral compositions.

For interactions between identical particles there is the possibility that exchange degeneracy enables particles in very different  $p$  states to still interact because of 'SOF swapping'. This can be seen by writing down the symmetric/antisymmetric form of the two-particle (eigenstate+perturbing particle) overlap integral. The SOF of the initial and final eigenstates could theoretically work together with the SOF of the eigenspectral components of the initial and final perturbing particle states to allow a  $p$ -crossing transition even when the SOF of the initial eigenstate is very different from the final. Optical thickness follows from such a particle interaction because low- $p$  eigenspectral components may then be transferred to more strongly interacting components. This possibility enables the prospect of limited interchange of baryons in dark states with traditional 'Maxwellian' matter during cosmic history. Potentially it offers a solution to the significant astrophysical problems of a continued source of star forming material in galaxies, the disk-halo conspiracy (mass distribution follows radial luminosity), the production of ionised gas from precessional galactic jets as observed in M42 at temperatures consistent with those expected from outer halo interactions, and the hot interacting gas in the Bullet cluster collision.

## 5. A formation scenario

A short account of the possible qualitative model of the formation of dark halos was given by Ernest (2006) and we summarise that approach here. There is still considerable work to be done in developing and testing the validity of the approach but the qualitative scenario does provide a general basis for how formation would need to proceed. Given the properties of particles in dark gravitational eigenstates, it is reasonable to expect that once particles have eigenspectral distributions that are dark, that, aside from for the types of particle interactions discussed above, they could largely remain in these distributions over cosmic times. Clearly the processes involved are dynamic and on-going, and the proportion of particles with dark eigenspectral distributions depends on the rates at which distributions are transferred back and forward between dark and visible states during cosmic history. Detailed calculations of these processes are potentially very difficult because not only do the transition rates depend on their closeness to the  $p=1$  diagonal, but the dynamic redistribution of matter concurrently changes the shape of the potential well and hence the overlap integrals involved in the rate calculations.

In the formation scenario proposed, each massive dark 'eigenstructure' halo is occupied by baryons and electrons in a self-assembled massive gravitational potential, each of which is initially seeded by the potential well of a supermassive black hole formed at the last,  $e^+/e^-$  phase transition at  $t \sim 0.75$  s in the early universe. Such black holes were themselves originally one of the first candidates proposed as a solution to the dark matter problem, but it was shown that their abundance could only provide up to  $10^{-7}$  of the closure density (Hall and Hsu, 1990). However in the present scenario we note that if a PBH is sufficiently large it can continue to accrete baryonic matter. Under normal circumstances this is countered by photon pressure via baryon-photon oscillation, but this process is critically dependent on the cross section for Compton scattering which is significantly reduced if the eigenspectral distribution of the captured baryons is biased toward dark states. In the present scenario therefore, the black holes formed at the last phase transition act as the seed potentials to capture baryons and electrons that then transfer to dark eigenspectral distributions thereby insulating them from the baryon-photon oscillation process and enabling them to add to the

captured baryonic dark halo, concurrently increasing the density contrast and well potential, and enhancing further matter capture in a continuing cycle.

It is well known that primordial black holes (PBH) can form from over-density regions at the various phase transitions in the early universe (Carr, 1975, Jedamzik and Niemeyer, 1999). It is expected that such black holes will form with masses up to the horizon mass  $M_H$  at the time of the phase transition. The PBHs required for eigenstructure seeding need to be massive and we are interested in the black holes formed at the  $e^+/e^-$  phase transition at  $t \sim 0.75$  s. Numerical calculations by Hawke and Stewart (2002) suggest a lower limit to  $M_{PBH}$  as  $\sim 10^{-4} M_H$  while Carr gives an approximate upper limit on PBH mass as

$$M_{PBH} \sim 1 M_S \left( \frac{T}{100 \text{ MeV}} \right)^{-2} \left( \frac{g_{\text{eff}}}{10.75} \right)^{-\frac{1}{2}} \quad (26)$$

where  $T$  is the temperature at the phase transition ( $\sim 1$  MeV at  $t \sim 0.75$  s),  $g_{\text{eff}}$  is the number of degrees of freedom (43/4 at the last phase transition) and  $M_S$  is the solar mass. This suggests a maximum black hole mass  $\sim 10^4 M_S$  while Afshordi et al (2003) consider up to  $10^6 M_S$ .

The capture of baryonic matter is in a sense similar to the capture of electrons by ions to form atoms and a simple version of the Saha equation

$$\frac{n_e n_i}{n_a (n_a - n_i)} = \frac{2 \pi m_e k T}{h^3} \exp \left( -\frac{E_i}{k T} \right) \quad (27)$$

suggests that particles might undergo a form of 'gravitational recombination' provided that the energy level concerned is deeper than the corresponding energy related to the temperature at the time involved. This fixes a particular radius within the seed well at which the condition  $|E_i| > f k T$  (where  $f \sim 2 - 10$ ) is satisfied. Ernest (2006) considered seed masses of between  $10^4$  and  $10^6 M_S$ , and derived an equation for the temporal development of a so-called thermal radius  $r_{th}$  at which this condition was satisfied:

$$\frac{\partial r_{th}(t)}{\partial t} - k_1 \frac{r_{th}(t)^3}{t^2} - \frac{r_{th}(t)}{2t} = 0 \quad (28)$$

where  $k_1$  is a constant relating to relevant parameters such as the effective enclosed mass, temperature etc., and the solution a function of  $r_{th}(t_0)$ , the initial size of the thermal radius (Ernest 2006). If the matter is effectively captured inside  $r_{th}$  then, as the surrounding universe expands and the temperature drops, the contrast density increases and  $r_{th}$  increases with time. Depending on the chosen value of  $f$ , results show that provided  $M_S \sim 5 \times 10^4 M_S$  or greater,  $r_{th}$  can increase rapidly (until equation 27 breaks down due to the presence of adjacent halos) and can accommodate a halo mass of  $10^{42}$  kg, generally before the completion of nucleosynthesis. Whether or not particles can effectively transfer to dark states within this time is still an open question because the model is still to be developed in detail and requires calculation of deep-state stimulated transition rates (the prevailing transition process in this strongly radiation-dominated era). It does suggest however that it might be possible to maintain consistency with measured nucleosynthesis ratios and still maintain baryonic densities applicable to the total matter content of the



universe: i.e. dark plus visible matter, either (1) because the baryons have transferred to weakly interacting states before nucleosynthesis completion or (2) because of the extreme inhomogeneity introduced by the eigenstructure halos. (Mass captured in the halos is sequentially removed from the more rapidly expanding, necessarily under-density, mid-halo regions as expansion proceeds.) Interestingly however, from Carr's black hole number density-mass spectrum equation, it can be calculated that the value  $r_{th}$  takes for the separation of such adjacent halos at the formation time translates, after universal expansion, into the order of magnitude for the number density of present day galaxies (Ernest, 2006).

In a traditional  $p^+/e^-$  recombining plasma once the temperature has dropped well below the ionisation level, virtually all electrons and protons have formed into atoms, so we might initially expect that today all the baryons and electrons of the universe would have gravitationally combined into halo eigenstructures and possibly also collapsed into dark eigenstates. There would then be no visible matter in the universe, particularly in the present scenario where halos grow until they overlap. During the formation process however, as discussed above there are weak, relatively 'field-free' corner regions in between adjacent halos and some baryons and electrons would have remained as thermalised distributions in these regions. The probability of any individual particle transferring to a dark state is necessarily small and so we expect that some as yet unknown fraction of matter in the halo itself as well as the matter in these field-free corner regions will form the basis of the visible matter we observe today. An interesting consequence from this is the prediction of the visible to total matter ratio. If we assume that halos fill space like oranges in a box and imagine that growth stops when the halo edges meet with the remaining matter left over in the corners then the ratio of this left over matter to the total matter should give us a ratio of the visible to total matter. Bertschinger (1985) has looked at the capture of baryonic matter by a central potential and has shown that such capture can result in self-similar density profiles which are reasonably consistent with the logarithmic potential,  $1/r^2$  profiles observed today. Assuming such a density profile, we get a ratio for visible to total matter of 0.23 for loose random packing and 0.186 for close random packing. This can be compared with the WMAP result which measures the visible to total matter ratio of the universe via baryon-photon oscillation as 0.18 (Tegmark et al., 2004).

It was estimated that initially the eigenstructure radius would have been formed from the horizon size  $\approx 3 \times 10^8 \text{ m}$  to  $\approx 10^{13} \text{ m}$ . It is expected that various processes would act on the eigenstates after baryonic capture. These would be required to expand the halos to their presently observed sizes. We imagine the matter at radius  $r \approx 10^{13} \text{ m}$  in a Maxwellian distribution which we approximate by a single momentum  $p = \sqrt{3mk_B T}$  (where  $k_B$  is Boltzmann's constant). Given an isotropic distribution of particles then particles enter the  $n, l$  diagram at a position that corresponds to their angular momentum. For the temperature conditions at initial formation this suggests the majority of particles will have values of  $l \sim r\sqrt{3mk_B T} / \hbar$  up to  $l \approx 8 \times 10^{22}$  for  $r \approx 3 \times 10^8 \text{ m}$ , ( $T \sim 10^{10} \text{ K}$ ) and  $l \approx 5 \times 10^{26}$  for  $r \approx 10^{13} \text{ m}$  ( $T \sim 4 \times 10^8 \text{ K}$ ).

We want to estimate the rate at which such particles might be promoted up or down via stimulated radiation processes. The stimulated transition rate is given by equation 24 which

depends on the overlap integral  $\Pi_{if}$  and on the energy density per unit angular frequency  $\rho(\omega_{if})$  at the transition frequency which relates to the temperature at the formation time. For  $T \sim 10^{10}$  K this peaks at  $\omega \sim 4 \times 10^{21}$  Hz, but this frequency corresponds to large changes in  $p$  values ( $\Delta l = \pm 1$ ) that do not have favourable  $\Pi_{if}$  values when the initial value of  $p(=p_i)$  is low. Hence there is an optimum value of  $\Delta n$  that will yield the maximum transfer rate. For smaller changes in  $p$  the value of  $\Pi_{if}$  is higher (for  $p_i = 1$  where  $\Delta p = 1$  necessarily, there is virtually 100% in-phase overlap in the dipole matrix element and  $\Pi_{if} \approx er$ ) but  $\rho(\omega_{if})$  is much smaller. Nevertheless at these high temperatures there is a peak rate  $\sim 10^{34} \text{ s}^{-1}$  that occurs for  $\Delta p = 1$  transitions originating on  $n_i = 1, p_i = 1$ . Likewise similar  $\Delta p = 1$  transitions originating on the deeper states where  $p_i \neq 1$  will show similar rates. Additionally however if the states are very deep, the rapid decrease in  $\Pi_{if}$  with increase in  $\Delta p$  (Ernest, 2009b) does not occur, and promotion demotion rates may be even greater. Thus although it was seen that the state dispersion due to radiation such as that from the CMB does not appreciably alter the relative eigenstate position on the state diagram for present day halos, in the early times of formation the rates are such that these halos could have been easily expanded. It is relatively easy to track the rates during cosmic history and indications are that radiation expansion of halos may have occurred up to as late in cosmic history as the beginning of the period of reionization. Although accurate calculations require detailed knowledge of the energy level spacings which have only recently been determined for logarithmic potentials. Further work is being carried out in this area.

## 6. Observations and predictions

It is difficult for any model of dark matter to predict observable phenomena because by the nature of dark matter it is not very observable! Perhaps the biggest departure of the present approach from traditional cosmic concordance is the early formation of massive eigenstructures. Whilst within the present theory traditional LCDM is left intact on the largest scales (indeed we know that eigenstructures themselves will function effectively in describing large scale structure as the original numerical modelling was carried out with similar mass 'particles'). One would anticipate that such a change would leave some imprint on for example the CMB. The halo separation at decoupling corresponds to fluctuations in the anisotropy spectrum at  $l \approx 10^4$ . Unfortunately at such high  $l$  values the finite time for atomic recombination has most likely smoothed out peaks due to the individual halos. One might see evidence in the Lyman- $\alpha$  forest, but since it is anticipated that every eigenstructure forms into a galaxy, this is really just noting the observed effects that galactic halos already have on the Lyman- $\alpha$  forest.

One possible observation might reveal the eigenstate nature of dark matter. We know that in the  $1/r^2$  density profiles the total energy of an eigenstate minus its potential energy is effectively a measure of its kinetic energy. This kinetic energy is constant with radius and determined only by eigenstate particle mass and the ratio  $M_0/R_0$ . Furthermore we know that although these high- $l$  eigenstates are very dark with respect to photon interactions, their interactions with other particles may not be so ineffective, because of relaxed selection rules. It is possible that dark baryons slowly 'leak' into the visible regime over time via collisions and interactions with particles and other eigenstates. If particle/dark-eigenstate collisions do occur then the eigenspectral distribution will shift to a lower- $l$ , visible composition. It is

suggested this is one of the primary origins of the hot x-ray gas seen in halos, and the radio and other emission from black hole jets as they precess in the halo and the hot x-ray emission seen in cluster collisions such as the famous “Bullet cluster”.

Firstly we note that the halo x-ray emission is at an approximately constant temperature across the radius of the halo, consistent with the radial dependence of the effective kinetic energy of eigenstates. The equivalent kinetic energy of these eigenstates averaged over the electron and proton component is most simply calculated from  $\bar{E}_K = GM_0(m_p + m_e)/4R_0$  which for the Milky Way corresponds to a temperature  $= 2\bar{E}_K / 3k_B = 1.3 \times 10^6$  K. The Milky Way exhibits a range of x-ray energies but the best estimates of the diffuse halo gas temperature are  $1.3 - 1.5 \times 10^6$  K (Kappes et al., 2003). If the hypothesis of energy transfer from dark to visible states is correct, one might expect to see, over a range of different halos, a linear correlation between two quantities  $M_0/R_0$  and the x-ray temperature, both of which should be measurable, the first by lensing and the second by x-ray satellites. In some halos a variation in velocity profiles with radius is observed and there might be a correlation between the halo temperature and the local the equivalent eigenstate kinetic energy as a function of radius within a single halo. It is also significant that some observed x-ray intensities mimic halo dark matter density profiles (ibid.) the generality of which could be tested.

## 7. Conclusion

Quantum theory predicts the existence of well-bound, dark gravitational eigenstates in potential wells like those associated with galactic or cluster halos. By allowing the possibility that these states could be incorporated into the eigenspectra of what would normally be visible elementary particles, it enables them to function as dark matter candidates. This then enables the nature and origin of dark matter to be understood without the need for new particles or new physics. Gravitational eigenstates have already been experimentally observed in the laboratory and there is no reason to deny their existence in large potential wells. Many of the properties of dark matter then arise as a natural consequence of (i) the functional properties of the wavefunctions corresponding to the dark eigenstates or (ii) the envisaged formation scenario.

Perhaps the most exciting aspect of gravitational eigenstates though will be realised if these states do turn out to be responsible for dark matter, for in doing this they will provide us not only with a solution to a long standing problem in astrophysics but also with a more generalised way to describe and understand the nature of matter on macroscopic scales.

## 8. References

- Afshordi, N., McDonald, P. and Spergel, D. N., (2003). Primordial Black Holes as Dark Matter: The Power Spectrum and Evaporation of Early Structures. *ApJ*, 594, pp. L71-L74
- Bernstein, D. H., Giladi, E. and Jones, K. R.W., (1998). Eigenstates of the gravitational Schrodinger equation. *MPLA*, 13, 29, pp. 2327-2336
- Bertschinger E., (1985). Self-similar secondary infall and accretion in an Einstein-de Sitter universe. *ApJS*. 58, pp. 39-66

- Carr B. J., (1975). The primordial black hole mass spectrum. *ApJ.*, 201, pp. 1-19. doi: 10.1086/153853
- Chavda, L. K. and Chavda, A.L., (2002). Dark matter and stable bound states of primordial black holes. *Class. Quantum Grav.* 19 2927 doi: 10.1088/0264-9381/19/11/311
- Chou C. H., Hu B. L. and Subaşı Y., (2011). Macroscopic quantum phenomena from the large N perspective, *J. Phys.: Conf. Ser.* 306 012002, doi: 10.1088/1742-6596/306/1/012002
- Ciftci, H., Ateser, E. and Koru, H., (2003). The power law and the logarithmic potentials. *J. Phys. A*, 36, 3821, (13 pp.), doi:10.1088/0305-4470/36/13/313
- Clowe, D., Bradač, M., Gonzalez, A. H., Markevitch M., Randall, S. W., Jones C. and Zaritsky, D., (2006). A Direct Empirical Proof of the Existence of Dark Matter, *ApJ* 648, L109, (5 pp.), doi: 10.1086/508162
- Colberg, J. M., White, S. D. M., Jenkins, A and Pearce, F. R., (1997). Linking cluster formation to large scale structure. arXiv:astro-ph/9711040v1. (6 pp.), Available from [http://arxiv.org/PS\\_cache/astro-ph/pdf/9711/9711040v1.pdf](http://arxiv.org/PS_cache/astro-ph/pdf/9711/9711040v1.pdf)
- Croft, R. A. C., and Efstathiou, G., (1993). Large-scale structure and motions from simulated galaxy clusters. astro-ph/9310016 11. (5 pp.), Available from [http://arxiv.org/PS\\_cache/astro-ph/pdf/9310/9310016v1.pdf](http://arxiv.org/PS_cache/astro-ph/pdf/9310/9310016v1.pdf)
- DeWitt, B. S. and Esposito, G., (2007). An introduction to quantum gravity. arXiv:hep-th/0711.2445v1., (68 pp.), Available from [http://arxiv.org/PS\\_cache/arxiv/pdf/0711/0711.2445v1.pdf](http://arxiv.org/PS_cache/arxiv/pdf/0711/0711.2445v1.pdf)
- Diemand, J. and Moore, B., (2009). The structure and evolution of cold dark matter halos. arXiv:astr-ph/0906.4340v1, (17 pp.), Available from [http://arxiv.org/PS\\_cache/arxiv/pdf/0906/0906.4340v1.pdf](http://arxiv.org/PS_cache/arxiv/pdf/0906/0906.4340v1.pdf)
- Doran, C., Lazenby, A., Dolan, S. and Hinder, I., (2005). Fermionic absorption cross section of a Schwarzschild black hole. *Phys. Rev. D*, 41, 124020, (6 pp.)
- Dvali, G., Gomez, C. and Mukhanov, S., (2011). Black Hole Masses are Quantized. arXiv:hep-ph/1106.5894v1, pp. 1-23, Available from [http://arxiv.org/PS\\_cache/arxiv/pdf/1106/1106.5894v1.pdf](http://arxiv.org/PS_cache/arxiv/pdf/1106/1106.5894v1.pdf)
- Ernest, A. D., (2001). Dark matter and galactic halos - a quantum approach. arXiv:astro-ph/0108319, pp. 1-53, Available from <http://arxiv.org/abs/astro-ph/0108319>
- Ernest, A. D., (2006). A Quantum approach to dark matter, In: *Dark Matter: New Research*, Ed J. Val Blain, pp. 91-147, NOVA Science Publishers, ISBN: 1-59454-549-9, New York
- Ernest, A. D., (2009a). Gravitational eigenstates in weak gravity I: Dipole decay rates of charged particles. *J. Phys. A: Math. Theor.* 42, 115207, (16 pp.)
- Ernest, A. D., (2009b). Gravitational eigenstates in weak gravity II: Further approximate methods for decay rates. *J. Phys. A: Math. Theor.* 42, 115208, (22 pp.)
- Feng, J. L., (2010). Dark Matter Candidates from Particle Physics and Methods of Detection. arXiv:astro-ph/1003.0904. (50 pp.), Available from [http://arxiv.org/PS\\_cache/arxiv/pdf/1003/1003.0904v2.pdf](http://arxiv.org/PS_cache/arxiv/pdf/1003/1003.0904v2.pdf)
- Gossel, G. H., Berengut, J.C. and Flambaum, V.V., (2010). Energy levels of a scalar particle in a static gravitational field close to the black hole limit. arXiv:gr-qc/1006.5541, (4 pp.), Available from <http://arxiv.org/abs/1006.5541>
- Hall, L. J. and Hsu, S. D., (1990). Cosmological production of black holes. *Phys. Rev. Lett.* 64, pp. 2848-2851, doi:10.1103/PhysRevLett. 64.2848

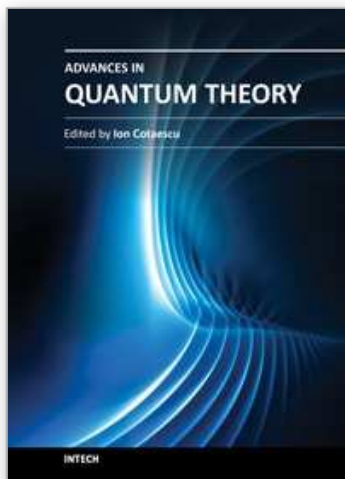


- Hawke, I. and Stewart, J. M., (2002). The dynamics of primordial black-hole formation. *Class. Quantum Grav*, 19, pp. 3687-3707, doi:10.1088/0264-9381/19/14/310
- Jaekel, M. T., Lamine, B., Lambrecht, A., Reynaud, S. and Maia Neto, P., (2006). Quantum decoherence and gravitational waves, In: *Beyond the Quantum*, Theo M Nieuwenhuizen et. al. (Eds.), pp. 125-134, Eproceedings, Lorentz Center Leiden, The Netherlands, May 29 - June 2, 2006, Eds., World Scientific, 10.1142/9789812771186\_0010
- Jedamzik, K. and Niemeyer, J. C., (1999). Primordial black hole formation during first-order phase transitions. *Phys.Rev.D*, 59, 124014, (7 pp.) doi:10.1103/PhysRevD.59.124014
- Kappes, M., Kerp, J. and Richter, P., (2003). The Composition of the Interstellar Medium towards the Lockman Hole. *A&A*, 405, pp. 607-616, doi: 10.1051/0004-6361:20030610
- Ketterle, W., (2002). Nobel lecture: When atoms behave as waves: Bose-Einstein condensation and the atom laser. *Rev. Mod. Phys.* 74, pp. 1131-1152
- Knebe, A., (1998). Virialisation of galaxy clusters in numerical simulations. arxiv.org/9811159v1 (12pp.) Available from [http://arxiv.org/PS\\_cache/astro-ph/pdf/9811/9811159v1.pdf](http://arxiv.org/PS_cache/astro-ph/pdf/9811/9811159v1.pdf)
- Kroupa, P., Famaey, B., de Boer, K. S., Dabringhausen, J., Pawlowski, M. S., Boily, C.M., Jerjen, H., Forbes, D., Hensler, G. and Metz, M. (2010). Local-Group tests of dark-matter concordance cosmology. *A&A*, 523, A32, (26 pp.) DOI 10.1051/0004-6361/201014892
- Lamine, B., Herve, R., Jaekel, M.T., Lambrecht, A. and Reynaud, S., (2011). Large-scale EPR correlations and cosmic gravitational waves. *EPL*, 95, 20004, (9 pp.)
- Milgrom, M., (1983). A modification of the Newtonian dynamics as a possible alternative to the hidden mass hypothesis. *ApJ* 270, pp. 365-370
- Nakamura, Y., Pashkin, Yu. A., and Tsai, J. S., (1999). Coherent control of macroscopic quantum states in a single-Cooper-pair box. *Nature* 398, pp. 786-788
- Nesvizhevsky V. V., Borner H. G., Petukhov A. K. et al., (2002). Quantum states of neutrons in the Earth's gravitational field. *Nature* 415, pp 297-9
- Primack, J. R., (2001). The nature of dark matter. arXiv:astro-ph/0112255 v1. (22 pp.) Available from [http://arxiv.org/PS\\_cache/astro-ph/pdf/0112/0112255v2.pdf](http://arxiv.org/PS_cache/astro-ph/pdf/0112/0112255v2.pdf)
- Reynaud, S., Maia Neto, P. A., Lambrecht, A. and Jaekel, M.-T., (2001). Gravitational decoherence of planetary motions. *Europhys. Lett*, 54, pp. 135-141. doi:10.1209/epl/i2001-00286-8
- Rovelli, C., (2008). Loop Quantum Gravity. *Living Rev. Relativity*, 11, 5, ISSN 1433-8351. Available from <http://www.livingreviews.org/lrr-2008-5>
- Rubin, V. and Ford, W. K. Jr., (1970). Rotation of the Andromeda Nebula from a Spectroscopic Survey of Emission Regions. *ApJ*. 159, pp. 379-403. doi:10.1086/150317
- Schiff, L. I., (1968). *Quantum Mechanics* (3<sup>rd</sup> Ed.), McGraw-Hill, ISBN-13: 978-0070856431, New York
- Schlosshauer, Maximilian A. (2007). *Decoherence and the Quantum-To-Classical Transition*, Springer, ISBN 978-3-540-35773-5
- Schmitt-Manderbach, T., Weier, H., Fürst, M., Ursin, R., Tiefenbacher, F., Scheidl, Th., Perdigues, J., Sodnik, Z., Rarity, J. G., Zeilinger, A. and Weinfurter, H., (2007).



- Experimental Demonstration of Free-Space Decoy-State Quantum Key Distribution over 144 km. *Phys. Rev. Lett.* 98, 010504, (4 pp.)
- Snowden, S.L., Freyberg, M.J., Kuntz, K.D., and Sanders, W.T., (2000). A Catalog of Soft X-Ray Shadows, and More Contemplation of the  $\frac{1}{4}$  keV Background. *ApJS*, 128, 171, (64 pp.), doi:10.1086/313378
- Tegmark, M. *et al.* [SDSS Collaboration], (2004). Cosmological parameters from SDSS and WMAP. *Phys. Rev. D* 69, 103501, (26 pp.)
- Vachaspati, T., (2009). Schrodinger Picture of Quantum Gravitational Collapse. *Class. Quantum Grav.* 26, 215007 (14 pp.), doi:10.1088/0264-9381/26/21/215007
- Van der Wal, Caspar H., ter Haar1, C. J., Wilhelm, F. K., Schouten, R. N., Harmans, C. J. P. M., Orlando, T. P., Lloyd, Seth and Mooij, J. E., (2000). Quantum Superposition of Macroscopic Persistent-Current States. *Science*, 290, no. 5492, pp. 773-777, DOI: 10.1126/science.290.5492.773
- Woodard, R. P., (2009). How far are we from the quantum theory of gravity? *Rep. Prog. Phys.* 72, 126002, (106 pp.), doi: 10.1088/0034-4885/72/12/126002
- Zbinden, H., Brendel, J., Tittel, W. and Gisin, N., (2001). Experimental test of relativistic quantum state collapse with moving reference frames. *J. Phys. A: Math. Gen.* 34, pp. 7103-7110, doi: 10.1088/0305-4470/34/35/334
- Zurek A.J., (1981). Pointer basis of quantum apparatus: Into what mixture does the wave packet collapse?, *Phys. Rev. D* 24, pp. 1516-1525.
- Zurek A.J., (1982). Environment-induced superselection rules. *Phys. Rev. D* 26, pp. 1862-1880.
- Zwicky, F., (1937). On the masses of nebulae and clusters of nebulae. *ApJ*. 86, pp. 217-246

IntechOpen



### **Advances in Quantum Theory**

Edited by Prof. Ion Cotaescu

ISBN 978-953-51-0087-4

Hard cover, 248 pages

**Publisher** InTech

**Published online** 15, February, 2012

**Published in print edition** February, 2012

The quantum theory is the first theoretical approach that helps one to successfully understand the atomic and sub-atomic worlds which are too far from the cognition based on the common intuition or the experience of the daily-life. This is a very coherent theory in which a good system of hypotheses and appropriate mathematical methods allow one to describe exactly the dynamics of the quantum systems whose measurements are systematically affected by objective uncertainties. Thanks to the quantum theory we are able now to use and control new quantum devices and technologies in quantum optics and lasers, quantum electronics and quantum computing or in the modern field of nano-technologies.

#### **How to reference**

In order to correctly reference this scholarly work, feel free to copy and paste the following:

Allan Ernest (2012). Gravitational Quantisation and Dark Matter, Advances in Quantum Theory, Prof. Ion Cotaescu (Ed.), ISBN: 978-953-51-0087-4, InTech, Available from:

<http://www.intechopen.com/books/advances-in-quantum-theory/gravitational-quantisation-and-dark-matter>

**INTECH**  
open science | open minds

#### **InTech Europe**

University Campus STeP Ri  
Slavka Krautzeka 83/A  
51000 Rijeka, Croatia  
Phone: +385 (51) 770 447  
Fax: +385 (51) 686 166  
[www.intechopen.com](http://www.intechopen.com)

#### **InTech China**

Unit 405, Office Block, Hotel Equatorial Shanghai  
No.65, Yan An Road (West), Shanghai, 200040, China  
中国上海市延安西路65号上海国际贵都大饭店办公楼405单元  
Phone: +86-21-62489820  
Fax: +86-21-62489821

© 2012 The Author(s). Licensee IntechOpen. This is an open access article distributed under the terms of the [Creative Commons Attribution 3.0 License](#), which permits unrestricted use, distribution, and reproduction in any medium, provided the original work is properly cited.

IntechOpen

IntechOpen